EPJ Web of Conferences **181**, 01008 (2018) https://doi.org/10.1051/epjconf/201818101008
*EXA2017*

# Single- and multi-nucleon $K^-$ interactions with nuclei near threshold

*Eliahu* Friedman[1,⋆] and *Avraham* Gal[1,⋆⋆]

[1] *Racah Institute of Physics, the Hebrew University, Jerusalem*

**Abstract.**
Six recent SU(3) chiral-model EFT approaches to the $\bar{K}$-nucleon interaction near threshold, constrained by $K^-p$ low-energy scattering and reaction data and by the kaonic hydrogen SIDDHARTA experiment, are used as input in kaonic atom calculations. Good agreement with the world-data on kaonic atoms is achieved with optical potentials built on the above models only when $\bar{K}N$ amplitudes are supplemented by a phenomenological multi-nucleon term. Comparing predictions with experimental single-nucleon absorption-at-rest fractions on nuclei, only two of the models together with their associated phenomenological term are acceptable. The information content of $K^-$-nucleus data near threshold is discussed and the topic of deeply-bound kaonic atoms is re-visited.

## 1 Introduction

The interaction of low energy $K^-$ mesons with nuclei received attention over the years mostly through analyses of experiments with kaonic atoms, see [1, 2] and references therein. Optical-model analyses of strong-interaction observables in kaonic atoms throughout the periodic table achieved fits of $\chi^2$ per point of less that 2 for the whole data put together, which is quite good considering that the data are from different experiments carried out in several laboratories. Advances with theoretical $\bar{K}N$ interaction near threshold, particularly with the $K^-p$ interaction constrained by experiment, raises the possibility of relating the optical potentials to the more fundamental interaction of $K^-$ with nucleons. However, attempts to construct optical potentials from $K^-$-nucleon scattering amplitudes showed that a significant phenomenological term must be included in the potential, which could be related to multi-nucleon processes. Very recently [3] we showed that out of six state-of-the-art models for the $K^-N$ amplitudes only two are able to reproduce experimental single-nucleon absorption fractions [4–6] on nuclei while also forming part of optical potentials that fit kaonic atoms data.

In the present work we extend the discussion of [3] with emphasis on the ratios between the two components of the potential. We discuss the radial sensitivity of kaonic atom experiments, focusing on various extrapolations of the potentials into the nuclear interior presented in earlier works. Finally we discuss the existence of deeply bound $K^-$ *atomic* states [7, 8] and whether they could provide additional information to that available from conventional kaonic atom experiments.

⋆e-mail: elifried@cc.huji.ac.il
⋆⋆e-mail: avragal@savion.huji.ac.il

## 2 Input amplitudes and optical potentials

Following Cieplý et al. [9] we consider in the present work six sets of $K^-N$ amplitudes derived in various strangeness $\mathcal{S}$=−1 chiral SU(3) meson-baryon coupled-channel dynamical model approaches at next-to-leading order (NLO). These models are constrained by fits to low-energy $K^-p$ scattering and reaction cross sections, to three precisely determined threshold branching ratios, and to the kaonic hydrogen energy shift and width measured by the SIDDHARTA Collaboration [10, 11]. With such potentials one can take a step forward beyond a purely phenomenological approach and construct an optical model based on a $t\rho$ formulation. All six sets of amplitudes display sharp dependence on energy near threshold making the potential very sensitive to the energy used in its construction. Here, as in recent years, we adopt a 'kinematical' approach where this energy is determined self-consistently [12–14]. In this approach the energy $\sqrt{s}$ and the amplitudes become functions of the nuclear density. Corrections due to Pauli correlations are also included [15]. For attractive optical potentials this energy is below threshold, $\sqrt{s} = M_N + M_{K^-} + \delta\sqrt{s}$, with $\delta\sqrt{s}$ <0.

Tab. 1 shows comparisons between calculation and experiment when the $t\rho$ optical potentials are based only on the $K^-N$ amplitudes as discussed above. Focusing on an average $K^-$-nucleus interaction, our approach is global, handling all the available experiments together, 65 data points from Li to U. As a test the table shows also results for a smaller set, consisting of kaonic atoms of P, S, Cl, Cu, Ag and Pb, where the experimental results are of particularly high quality. It is evident that in all cases there is no agreement between experiment and calculation. Similar conclusions have been obtained in earlier studies of kaonic atoms.

**Table 1.** $\chi^2$ values for 65 kaonic atom data points and for a sub-set of 18 points, obtained with optical potentials based only on six $K^-N$ amplitudes discussed here (see [3, 9] for notation). The 65 points represent the world data for kaonic atoms. The 18 points are for six species of kaonic atoms where the experimental results are particularly comprehensive, see text.

| model | B2 | B4 | M1 | M2 | P | KM |
|---|---|---|---|---|---|---|
| $\chi^2$(65) | 1174 | 2358 | 2544 | 3548 | 2300 | 1806 |
| $\chi^2$(18) | 364 | 733 | 949 | 1232 | 480 | 449 |

In order to obtain good fit to experiment, a phenomenological term is added to the single-nucleon based amplitude, namely, we add a term $B(\rho/\rho_0)^\alpha$ and vary the three parameters Re$B$, Im$B$ and $\alpha$, with $\rho_0$ the central nuclear density. The fits obtained in that way are as good as with purely phenomenological potentials. Due to obvious correlations between $\alpha$ and $B$ we eventually grid on the former, and Tab. 2 shows typical results. As noted in the Introduction, a $\chi^2$ per point of less than 2 is considered most acceptable for such global fits to large and diverse data sets.

The additional term $B(\rho/\rho_0)^\alpha$ in the amplitude may be considered as representing multi-nucleon processes. Note that for $\alpha$ =1, a formal dependence of the *potential* on $\rho^2$ has traditionally been referred to as representing two-nucleon processes. In particular, Im$B$ represents absorptions on two nucleons, which are the pion-less absorptions known well from experiment. Consequently, fits resulting in negative values for Im$B$ must be rejected.

Tab. 3 shows results for the P and KM potentials supplemented by their respective $B(\rho/\rho_0)^\alpha$ term. It is seen that for $\delta\sqrt{s}$=0, i.e. using single-nucleon amplitudes at threshold, the solutions are unacceptable on account of negative Im$B$. Similar results and significantly larger values of $\chi^2$ are found for the other four sets of amplitudes when $\delta\sqrt{s}$=0. We also note that the results for the P and KM options are essentially the same, within errors. From the results shown in tables 2 and 3 it is not possible to prefer one model to the other, neither on the basis of quality of fits nor from values of the exponent

**Table 2.** Results of best-fits to 65 and 18 data points when the six amplitudes are supplemented by a complex empirical term $B(\rho/\rho_0)^\alpha$ with $\alpha$ fixed by separate fits, see text.

| model | B2 | B4 | M1 | M2 | P | KM |
|---|---|---|---|---|---|---|
| $\chi^2(65)$ | 111 | 105 | 121 | 109 | 125 | 123 |
| $\alpha$ | 0.3 | 0.3 | 0.3 | 1.0 | 1.0 | 1.0 |
| Re$B$ (fm) | 2.4±0.2 | 3.1±0.1 | 0.3±0.1 | 2.1±0.2 | −1.3±0.2 | −0.9±0.2 |
| Im$B$ (fm) | 0.8±0.1 | 0.8±0.1 | 0.8±0.1 | 1.2±0.2 | 1.5±0.2 | 1.4±0.2 |
| $\chi^2(18)$ | 17 | 15 | 19 | 17 | 17 | 16 |
| $\alpha$ | 0.3 | 0.3 | 0.3 | 1.0 | 1.0 | 1.0 |
| Re$B$ (fm) | 2.7±0.3 | 2.9±0.1 | 0.3±0.1 | 2.2±0.2 | −1.3±0.2 | −0.9±0.3 |
| Im$B$ (fm) | 0.8±0.2 | 0.8±0.1 | 0.6±0.1 | 1.1±0.2 | 1.4±0.3 | 1.3±0.3 |

**Table 3.** Results of best-fits to the full data set with the P and the KM amplitudes supplemented by a complex empirical term $B(\rho/\rho_0)^\alpha$ with $\alpha$ fixed, using either the sub-threshold prescription for variable $\delta\sqrt{s}$ (var.) or on-threshold values ($\delta\sqrt{s}$=0).

| model | P | KM | P | KM | P | KM |
|---|---|---|---|---|---|---|
| $\chi^2(65)$ | 135 | 139 | 125 | 123 | 125 | 122 |
| $\delta\sqrt{s}$ | 0 | 0 | var. | var. | var. | var. |
| $\alpha$ | 1 | 1 | 1 | 1 | 2 | 2 |
| Re$B$ (fm) | −1.9±0.1 | −1.8±0.1 | −1.3±0.2 | −0.9±0.2 | −0.5±0.6 | 0.3±0.7 |
| Im$B$ (fm) | −0.8±0.1 | −1.1±0.1 | 1.5±0.2 | 1.4±0.2 | 4.6±0.7 | 3.8±0.7 |

$\alpha$. Additional experimental information is required and that is available as single-nucleon absorption fractions.

## 3 Single-nucleon absorption fractions

Based on fractions of $K^-$ absorption-at-rest on several nuclear species measured many decades ago, it is possible to distinguish between the six models discussed in the present work [3]. The level width $\Gamma$ of a kaonic atom state which is usually obtained from the complex eigenvalue $E_{K^-} - i\Gamma/2$ when solving the Klein-Gordon equation with an optical potential $V_{K^-}$, is also related to the imaginary part of the potential by the overlap integral of Im $V_{K^-}$ and $|\psi|^2$,

$$\Gamma = -2 \frac{\int \mathrm{Im}\, V_{K^-}\, |\psi|^2\, d\vec{r}}{\int [1 - (B_{K^-} + V_\mathrm{C})/\mu_K]\, |\psi|^2\, d\vec{r}}, \tag{1}$$

where $B_{K^-}$, $V_\mathrm{C}$ and $\mu_K$ are the $K^-$ binding energy, Coulomb potential and reduced mass, respectively, and $\psi$ is the $K^-$ wave function of the particular state concerned. Partial widths for absorption on a single nucleon and in a multinucleon process are easily calculated for the best fit potentials using the single-nucleon based amplitudes and the corresponding phenomenological additional term.

From the three bubble-chamber experiments mentioned in the introduction [4–6] we adopt a fraction of 0.75±0.05 for the single-nucleon absorption-at-rest of $K^-$ on nuclei heavier than C. Fig. 1 shows very good agreement between calculations and experiment for amplitudes P and KM, supplemented by a phenomenological term. The two models are indistinguishable on this figure. The small

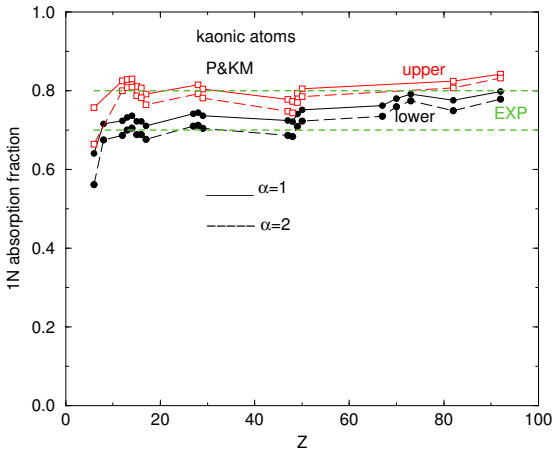


**Figure 1.** Fractions of single-nucleon absorption for amplitudes P and KM: solid circles are for lower states, open squares for upper states, solid curves use $B$ values from Tab. 3 for $\alpha$=1, long-dashed curves use $B$ values for $\alpha$=2. Horizontal dashed lines mark the range of experimental values of the single-nucleon absorption fraction. Models P and KM are indistinguishable from each other on this figure.

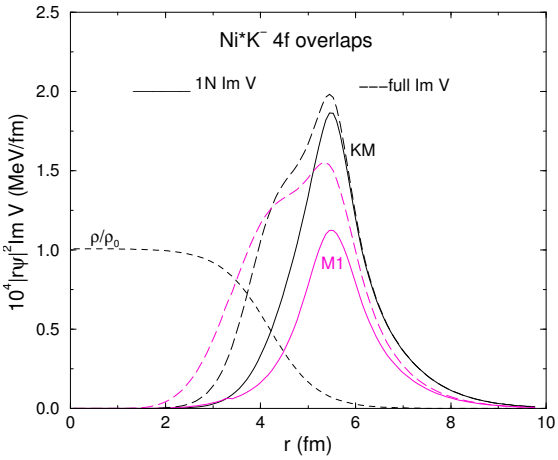


**Figure 2.** Overlaps of the absolute value squared of the 4f radial wave function in kaonic atoms of Ni with the imaginary part of the optical potential based on the KM amplitude and on the M1 amplitude. Solid lines for potentials due to the $K^-N$ amplitudes; dashed line for the corresponding full potentials including a phenomenological term. Also shown is the relative density for Ni.

dependence on the choice of $\alpha$ is evident. From the radiative widths of the transitions concerned one concludes that about 80% of absorptions take place from the lower states, except for C where most of the absorptions are from the upper state. The other four sets of amplitudes lead to calculated single-nucleon absorption fractions of 0.4-0.6, in disagreement with experiment.

Fig. 2 shows examples for the overlaps of the 4f state in kaonic atoms of Ni. It is easily seen that whereas for the KM amplitudes the area under the single-nucleon curve is about 75% of the area under the full amplitude curve, the corresponding ratio for the M1 amplitudes is only 50%. However, both provide equally good fit to the kaonic atom observables for Ni, and only the absorption fractions distinguish between these models.

## 4 $K^-$ potentials vs. density

Fig. 3 shows examples of the full amplitudes (single nucleon plus a phenomenological term) for $K^-$ interacting with Ni obtained from global fits to kaonic atoms, based on the P and the KM models. Here the single-nucleon amplitudes are supplemented by a phenomenological term with the exponent $\alpha$ equals 1 (P1 and KM1) or 2 (P2 and KM2), as given in Tab. 3. The full amplitudes are seen to be dominated by the $K^-N$ input at low densities and then the different models produce different amplitudes as the density increases towards the nuclear interior. This is particularly so for the real part of the amplitudes, whereas the imaginary part remains almost model-independent up to about 50% of the central density. The similarity between the P-based and the KM-based amplitudes is clearly seen on this figure.

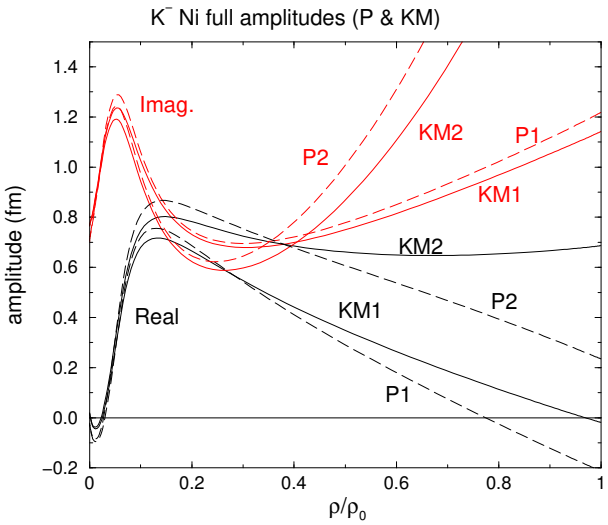


**Figure 3.** Examples for the full $K^-$Ni amplitudes (single nucleon plus a corresponding phenomenological term). In black for the real part, in red for the imaginary. P (dashed) and KM (solid lines) are the Prague and Kyoto-Munich models. The 1 and 2 refer to $\alpha$=1 and 2, respectively, in the phenomenological term.

A more transparent picture emerges from the optical potentials. Fig. 4 shows optical potentials for $K^-$ on Ni from global fits to kaonic atoms data that are based on a theoretical $K^-N$ amplitude plus a phenomenological term and, in addition, agree with single-nucleon absorption fractions. Also shown is a corresponding purely phenomenological optical potential producing similarly good fit to kaonic atom data. Obviously with this type of potential absorption ratios are meaningless and the values at low density are unconstrained by a low density limit. The real parts of the potentials for the four models agree with each other up to about 25% of the central density. The imaginary part is seen to

be well-determined up to 50% of the central density, reflecting the observation that strong interaction effects in kaonic atoms are dominated by the imaginary potential where level widths are significantly larger than shifts. It is concluded that at larger densities the various models produce just analytical continuations from values close to the nuclear surface. Note that the present extrapolated imaginary potentials are deeper than the purely phenomenological values.

The depth of the real potential was a topic of some controversy. Fig. 4 suggests that the behaviour at very low densities determines the extrapolation to larger densities. Indeed it is seen that in contrast to the purely phenomenological potential that has a smooth dependence on density, the other potentials have some structure near the surface and hence extrapolate differently to the nuclear interior, see [3] for further details.

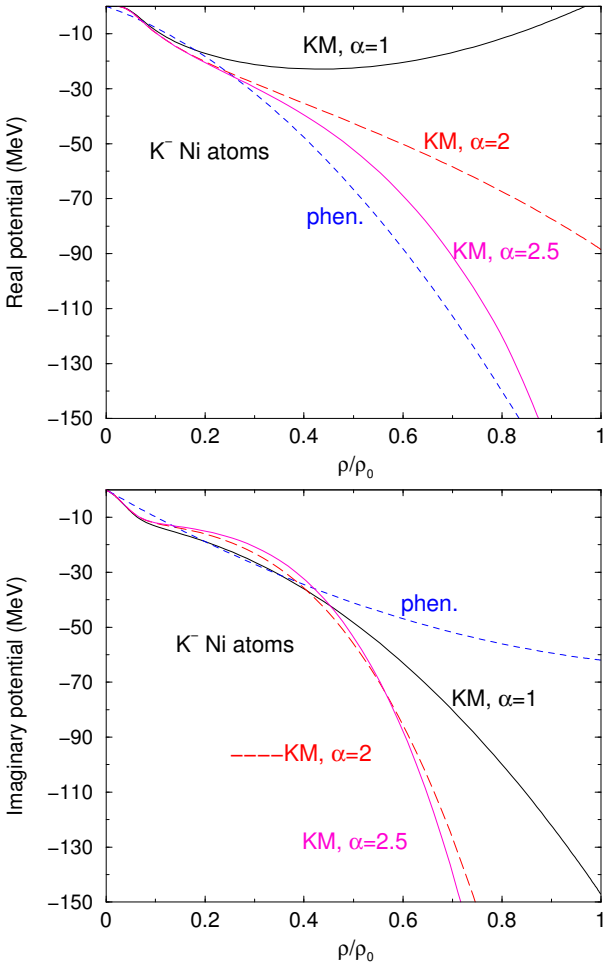


**Figure 4.** Real part (top) and imaginary part (bottom) of best-fit $K^-$Ni optical potentials based on the KM single nucleon amplitudes plus a phenomenological term with $\alpha$=1, 2 and 2.5 in the phenomenological term. Also shown is a purely phenomenological potential

## 5 Deeply bound kaonic atom states

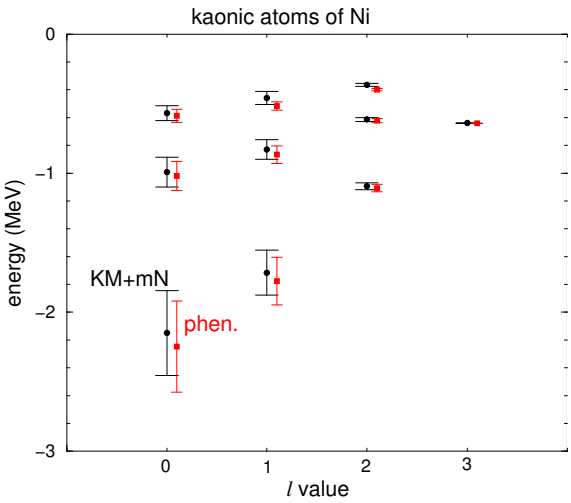


**Figure 5.** Energy levels of kaonic atom of Ni, showing the energies and the full widths. In red calculated for a purely phenomenological best-fit potential [7, 8], in black for the KM plus phenomenological best-fit potential for the KM model with $\alpha$=1.

Finally we discuss the possible existence of 'deeply bound' kaonic atom states, i.e. deep atomic states which are not populated by the usual cascade of X-rays. These states have been predicted [7, 8] two decades ago but no attempts have been made to observe them experimentally. It is instructive to follow briefly the history of the deeply bound pionic atoms, observed experimentally for the first time by Yamazaki et al. [16].

The first prediction that the deepest pionic atom states in heavy nuclei are sufficiently narrow to make them observable was by Friedman and Soff in 1985 [17]. The explanation given was the repulsion of the *atomic* wave function from the nucleus due to the strong *s*-wave repulsive term, thus reducing the overlap with the nucleus and causing the widths of the levels to be small. Three years later Toki and Yamazaki [18] discussed also methods for populating such states, which eventually led to the observation in 1996 [16]. It turned out that the strong interaction level shifts and widths of the deeply bound states were in agreement with predictions made with empirical pionic atom potentials based on the broad data-base of conventional states [19]. In particular, the enhancement within the nucleus of the *s*-wave isovector term of the pion-nucleus potential was found to agree with what had already been known from global analyses of pionic atoms [20]. We expect similar situation for kaonic atoms.

Fig. 5 shows positions and widths of energy levels in kaonic atom of Ni, calculated from a purely phenomenological potential [7] and from the current KM ($\alpha = 1$) potential. The results are almost identical for the two models, displaying very small sensitivity to detail, *provided* the potential fits the entire data on kaonic atoms. The mechanism in kaonic atoms is the *effective* repulsion due to strong absorption, which is operative when the absorption is confined to a relatively small region of the atom.

Fig. 6 shows overlaps of atomic wave functions with the Ni nucleus for the observed 4f state and for the predicted 1s state. The absolute scales differ by three orders of magnitudes and so do the widths, about one keV compared to one MeV, but the depth of penetration into the nucleus are the

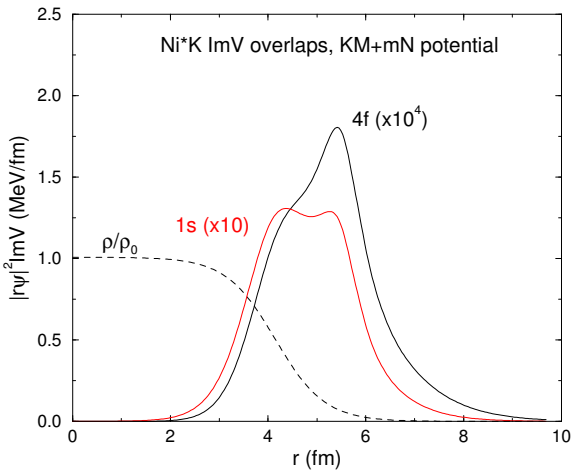


**Figure 6.** Overlaps of the absolute value squared of the 4f and 1s radial wave function in kaonic atoms of Ni with the imaginary part of the optical potential based on the KM amplitudes plus a phenomenological part with $\alpha$=1. Also shown is the relative density of the nuclear density of Ni.

same. It therefore appears that deeply bound kaonic atom states will not provide information on the interior different from what is known from conventional states.

## 6 Summary

With six state-of-the-art models providing $K^-N$ amplitudes near threshold it is found, as expected, that empirical terms must be added in each case to produce fit to the world's data on strong interaction effects in kaonic atoms. The six models appear equivalent on this basis, but when the fraction of absorption-at-rest on single nucleons is considered, then only two of the models, the Prague (P) and the Kyoto-Munich (KM) model, pass the test. Comparing amplitudes and potential details from the various acceptable versions, it is concluded that the real potentials are well determined only for densities up to 25% of the central density. Imaginary potentials display better penetration into the nuclear interior, being well determined up to 50% of the central density.

Re-visiting the topic of deeply bound kaonic atoms, we find that such states are well-defined but they are hardly sensitive to details of the potentials, once these are obtained from best-fits to conventional kaonic atoms data. It is concluded that the limited overlap of wave functions with the nucleus, that is the mechanism making these states sufficiently narrow, is the mechanism limiting sensitivities of kaonic atom experiments to only relatively small densities.

## References

[1] C.J. Batty, E. Friedman, A. Gal, Phys. Rep. **287** 385 (1997)
[2] E. Friedman, A. Gal, Phys. Rep. **452** 89 (2007)
[3] E. Friedman, A. Gal, Nucl. Phys. A **959** 66 (2017)
[4] H. Davis, F. Oppenheimer, W.L. Knight, F.R. Stannard, O. Treutler, Nuovo Cimento **53A** 313 (1968)

[5] J.W. Moulder, N.E. Garrett, L.M. Tucker, W.M. Bugg, G.T. Condo, H.O. Cohn, R.D. McCulloch, Nucl. Phys. B **35** 332 (1971)
[6] C. Vander Velde-Wilquet, J. Sacton, J.H. Wickens, D.N. Tovee, D.H. Davis, Nuovo Cimento **39A** 538 (1977)
[7] E. Friedman, A. Gal, Phys. Lett. B **459** 43 (1999)
[8] E. Friedman, A. Gal, Nucl. Phys. A **658** 345 (1999)
[9] A. Cieplý, M. Mai, U.-G. Meißner, J. Smejkal, Nucl. Phys. A **954** 17 (2016)
[10] M. Bazzi, et al. (SIDDHARTA Collaboration), Phys. Lett. B **704** 113 (2011)
[11] M. Bazzi, et al. (SIDDHARTA Collaboration), Nucl. Phys. A **881** 88 (2012)
[12] A. Cieplý, E. Friedman, A. Gal, D. Gazda, J. Mareš, Phys. Lett. B **702** 402 (2011)
[13] A. Cieplý, E. Friedman, A. Gal, D. Gazda, J. Mareš, Phys. Rev. C **84** 045206 (2011)
[14] E. Friedman, A. Gal, Nucl. Phys. A **899** 60 (2013)
[15] T. Waas, M. Rho, W. Weise, Nucl. Phys. A **617** 449 (1997)
[16] T. Yamazaki, R.S. Hayano, K. Itahashi, K. Oyama, A. Gillitzer, H. Gilg, M. Knülle, M. Münch, P. Kienle, W. Schott, H. Geissel, N. Iwasa, G. Münzenberg, Z. Phys. A **355** 219 (1996)
[17] E. Friedman, G. Soff, J. Phys. G: Nucl. Phys. **11** L37 (1985)
[18] H. Toki, T. Yamazaki, Phys. Lett. B **213** 129 (1988)
[19] E. Friedman, A. Gal, Phys. Lett. B **432** 235 (1998)
[20] E. Friedman, A. Gal, Nucl. Phys. A **724** 143 (2003)